Bandwidth-driven nature of the pressure-induced metal state of LaMnO3

Aline Y. Ramos, Narcizo M. Souza-Neto, Hélio C. N. Tolentino, Oana Bunau, Yves Joly, Stéphane Grenier, Jean-Paul Itié, Anne-Marie Flank, Pierre Lagarde, Alberto Caneiro

Bandwidth-driven nature of the pressure-induced metal state of $LaMnO_3$

2011 EPL 96 36002

(http://iopscience.iop.org/0295-5075/96/3/36002)

A Letters Journal Exploring the Frontiers of Physics

November 2011

EPL, **96** (2011) 36002
doi: 10.1209/0295-5075/96/36002

www.epljournal.org

Bandwidth-driven nature of the pressure-induced metal state of $LaMnO_3$

A. Y. Ramos[1(a)], N. M. Souza-Neto[2,3], H. C. N. Tolentino[1], O. Bunau[1], Y. Joly[1], S. Grenier[1], J.-P. Itié[4], A.-M. Flank[4], P. Lagarde[4] and A. Caneiro[5]

[1] *Institut Néel, CNRS et Université Joseph Fourier - BP 166, F-38042 Grenoble Cedex 9, France, EU*
[2] *Advanced Photon Source, Argonne National Laboratory - Argonne, IL 60439, USA*
[3] *Laboratório Nacional de Luz Síncrotron - P.O. Box 6192, 13084-971, Campinas, São Paulo, Brazil*
[4] *Synchrotron SOLEIL - L'Orme des Merisiers, Saint-Aubin, BP 48, 91192 Gif-sur-Yvette Cedex, France, EU*
[5] *Centro Atómico Bariloche, CNEA and Universidad Nacional de Cuyo - 8400 S.C. de Bariloche, Argentina*

received 11 July 2011; accepted in final form 8 August 2011
published online 17 October 2011

PACS 61.50.Ks – Crystallographic aspects of phase transformations; pressure effects
PACS 71.70.Ej – Spin-orbit coupling, Zeeman and Stark splitting, Jahn-Teller effect
PACS 71.30.+h – Metal-insulator transitions and other electronic transitions

Abstract – Using X-ray absorption spectroscopy (XAS), we studied the local structure in $LaMnO_3$ under applied pressure across and well above the insulator-to-metal (IM) transition. A hysteretic behavior points to the coexistence of two phases within a large pressure range (7 to 25 GPa). The ambient phase with highly Jahn-Teller (JT) distorted MnO_6 octahedra is progressively substituted by a new phase with less-distorted JT MnO_6 units. The electronic delocalization leading to the IM transition is finger-printed from the pre-edge XAS structure around 30 GPa. We observed that the phase transition takes place without any significant reduction of the JT distortion. This entails band overlap as the driving mechanism of the IM transition.

$LaMnO_3$ is the parent compound of a family of doped manganates that exhibit a multitude of electronic phases and unusual properties with strong potential for new electronic devices [1]. The compound crystallizes in the orthorhombically distorted perovskite structure (space group *Pbmn*), in which every Mn^{3+} ion with high-spin configuration $t_{2g}^3 e_g^1$ is surrounded by an octahedron of six oxygen ligands. Under ambient conditions, the Jahn-Teller (JT) instability of the singly occupied e_g orbitals gives rise to cooperative distortions of the MnO_6 octahedra, which induce orbital ordering and may be responsible for the insulating behavior of $LaMnO_3$. Although the ground-state of $LaMnO_3$ can be explained both by cooperative JT distortion and orbital exchange interaction, their relative importance lead to different physics for the doped systems and is then an important issue for predicting and optimizing physical properties. However, the separation of the two effects is a very delicate issue [2–8] that calls for accurate experimental probes.

At ambient pressure $LaMnO_3$ undergoes at $T_{IM} = 710$ K an insulator-to-metal (IM) transition, structurally described as a transition from an ordered toward a disordered array of JT distorted octahedra. The long-range structure is characterized by a strong cell symmetrization and the loss of the orbital order [9]. The local scale JT splitting persists essentially unaltered across the IM transition, which is marked by the symmetrization of the thermal fluctuations in the distorted MnO_6 units [10,11]

At ambient temperature, transition towards a metal state can also be attained by application of external hydrostatic pressure. High pressure reduces lattice parameters, favoring orbital overlap and concomitant enhancement of electron delocalization. It also forces an atomic rearrangement, tending to reduce lattice distortions (inter-octahedral and intra-octahedra rearrangements). In $LaMnO_3$ the IM transition has been reported by Loa and coworkers at an applied pressure of 32 GPa [12]. Using X-ray diffraction under pressure, these authors obtained refined atomic positions up to 11 GPa [12]. From an extrapolation of their results, they predict that the local JT distortion should completely vanish around 18 GPa. However, in a previous X-ray absorption spectroscopy (XAS) study under pressures up to 15 GPa [13], our group observed a shortening of the long MnO bond lenght too limited to lead to a

(a) E-mail: aline.ramos@grenoble.cnrs.fr

quenching of the JT distortion at 18 GPa, contradicting those predictions. Also by an extrapolation, it was deduced that a total removal of the JT distortion would occur only for pressures around 30 GPa, close to the onset of metallization. Importantly, when the pressure was released from 15 GPa down to 9 GPa, an incomplete recovering of the structural environement aroused suspicion of a possible phase coexistence in this pressure range. Phase coexistence are not unusual in perovskite material. It has been observed in $LaMnO_3$ at high temperature [14,15] and even suggested at high pressures [12,16,17]. Recently, Baldini and coworkers [18] have pointed out the persistence of the JT distortion coexisting with a new emergent undistorted phase up to 32 GPa. Besides its importance for the thermodynamics of the transition, a phase coexistence may completely invalidate any extrapolation of the experimental data at higher pressures and revoke previous conclusions about the vanishing of JT distortion in the metallic phase.

In this letter we investigate by XAS the local structure in $LaMnO_3$ under applied pressures across and well-above the IM transition. XAS is a local probe, mostly affected by the short- and medium-range environment of a selected atom and sensing short time scale. There have been various XAS works shedding light on the nature of the Jahn-Teller distortion, electronic states, thermal behavior, and disorder in manganites [11,19–23]. The main parameters involved are the local coordination around Mn atoms (Mn-O distances and distribution) and some slight modifications on the octahedra arrangement. A consistent analysis of the nearest neighbors does not necessarily require an *a priori* knowledge of the long-range arrangement, being otherwise able to provide masked details of the local structure. We observe an hysteretic behavior that points to the coexistence of two phases within a large pressure range (7 to 25 GPa). The ambient phase with largely JT distorted MnO_6 units coexist over a large range of pressure with a new phase with more regular but still distorted MnO_6 units. The IM transition takes place within this latter distorted phase, without any significant reduction of the local JT distortion. Metallization turns out to be unconnected with vanishing of the local distortion. Our study then provides experimental evidences of a bandwidth-driven nature of the pressure-induced insulator-to-metal transition in $LaMnO_3$.

High-pressure XAS measurements at the Mn K-edge (6539 eV) were performed at LUCIA beamline [24] hosted at the Swiss Light Source. The $LaMnO_{3.00}$ poly-crystal was synthesized following an experimental procedure enabling an accurate control of the oxygen stoichiometry [25]. The monochromatic beam was focused to a $5 \times 5\,\mu m^2$ spot in a perforated diamond anvil cell (DAC) with silicone oil as pressure-transmitting medium. The non-hydrostatic components of this medium may lead to large pressure deviations, up to 5% over a diameter of 50 μm for pressures above 15 to 30 GPa [26,27]. However, it becomes negligible in our experimental conditions

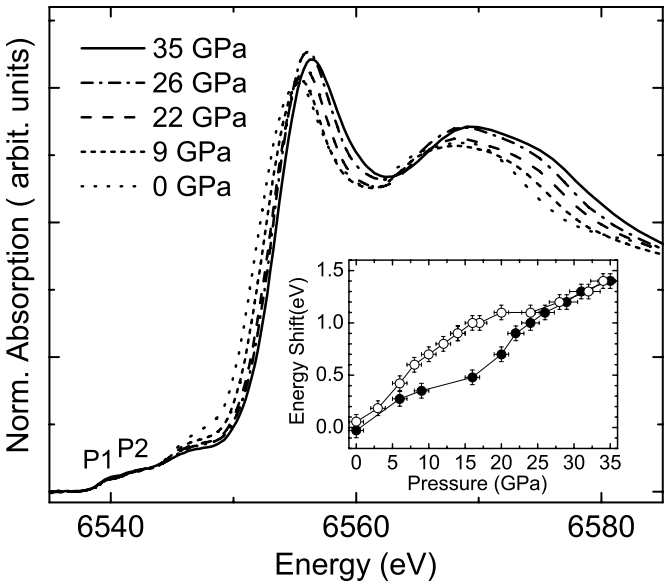

Fig. 1: (a) Mn K-edge XANES spectra for $LaMnO_3$ for selected pressures. The shift in the edge position is associated to the reduction of the Mn-O long bond. The increase in the white line (6555 eV) corresponds to a decrease in JT splitting. Inset: edge shift as a function of the applied pressure, for increasing pressure (plain symbols) and decreasing pressure (open symbols).

where the highly focused beam probes a small surface of $5 \times 5\,\mu m^2$. The pressure was *in situ* calibrated using the luminescence of a single ruby chip nearly the DAC center, with an accuracy of ≈ 0.3 GPa. An error bar of 5%, is estimated for the absolute pressure scale due to the separation of the probed area and the ruby positions. Using a gas membrane-driven mechanism, the pressure was increased step by step up to 35 GPa, well above the expected IM transition, then released by steps down to ambient pressure. EXAFS (Extended X-ray Absorption Fine Structure) data were collected up to about 8 $Å^{-1}$ in photo-electron wave number. The near-edge spectra (XANES) were normalized between 150 and 250 eV above the edge. The sample thickness was checked throughout the experiment and the normalization corrects for a small sample thickness reduction with pressure. During a sequence of XANES experiments, the energy shift was carefully monitored by recurrent collections of the XANES spectrum of a Mn metal foil (edge in 6539.1 eV). Moreover, the energy scale was verified after releasing the pressure down to the ambient conditions; energy scale stability as small as 0.1 eV were certified. The pre-edge and XANES features were compared to *ab initio* full multiple scattering calculations using the FDMNES code [28] for 6.5 Å large clusters using structural data of $LaMnO_3$ under ambient conditions in the *Pbnm* structure [9].

Figure 1 shows the Mn K-edge XANES at a few representative pressures. The most striking features are the continuous shift of the absorption threshold towards

higher energies and the enhancement of the white line (6555 eV). Due to the selection rules in X-ray absorption spectroscopy the K-edge transition originates from the core 1s state to the projected np (mainly 4p) unoccupied density of states (DOS). XAS probes the partial-DOS modified by the presence of the 1s core hole that sorts out the 4p states around the Mn site from the ground-state band structure. The white line position and threshold depends then essentially on the Mn-O bonds. The enhancement in the white line accounts for the increasing overlap of the wave functions imposed by hydrostatic pressure. Such enhancement, well reproduced by *ab initio* simulations, indicates a reduction of the local distortion of the Mn sites [13]. These outcomes show qualitatively that the short bonds $(\text{Mn-O})_s$ are less reduced than the long $(\text{Mn-O})_l$ ones by the application of an external pressure, in agreement with X-ray diffraction measurements [12,29]. As the manganese formal valence keeps unchanged, the edge shift (δE) expresses modifications in the repulsive nearest neighbors potential arising from shortening the Mn-O bonds in the coordination shell [30]. Besides, as shorter bond lengths correspond to higher edge energies, the edge threshold is determined by the long bond length $(\text{Mn-O})_l \approx 2.15$ Å. Indeed, the expected energy shift corresponding to the different long and short distances ($\delta R \approx 0.2$ Å) is about 2 eV [31]. The evolution δE of the edge threshold as a function of the applied pressure (inset fig. 1) is then essentially related to the specific reduction in this long bond [13]. The overall shift of $\delta E = +1.5$ eV corresponds to a reduction of $\backsimeq 0.15$ Å in bond length. The edge shifts strongly between 15 and 25 GPa when pressure is increased but, when the pressure is released, a well-defined hysteresis is observed (inset fig. 1). To recover the edge energy of the initial point at 15 GPa, the pressure has to be released down to about 5 GPa. Even if some deviatoric stress effects might exist and lead to some strain in the small poly-crystalline grains [26,27], these effects should be smaller than the observed bond length hysteresis (≈ 0.05 Å or 2.5%) in the 10 to 15 GPa range. Zhao and coworkers [32] found in a similar compound a highest strain difference of 0.3% at 6 GPa originating from silicone oil at non-hydrostatic conditions. XAS probes the local coordination around Mn atoms, and is not measuring directly different phases. The hysteresis provides an indirect evidence of the occurrence of mixed phases over a large pressure range. Such hysteresis characterizes the first-order nature of a phase transition where an activation barrier has to be overcome, causing the formation of domains around nucleation centers. The spatial (domain size) and temporal scales of these domains are probably too small to be observed by diffraction techniques. Several papers in the literature relate the presence of an hysteresis to the existence of phase mixing in similar compounds [23,33–35]. The occurrence of mixed phases in $LaMnO_3$ under pressure has already been pointed out by Baldini and coworkers [18] in a similar pressure range. They identified peaks in the Raman spectra related to phonon modes involving oxygen ions and a gradual transfer of spectral weight from one phase to another.

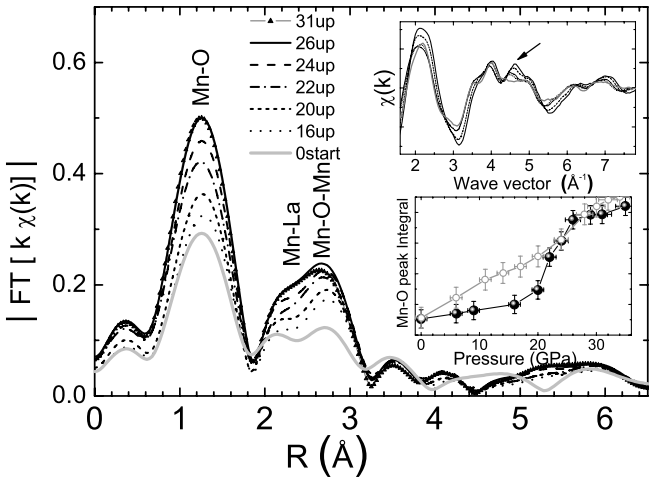

Fig. 2: Fourier Transform of the EXAFS signal for $LaMnO_3$ for selected pressures. Upper inset: EXAFS signal. Lower inset: evolution of the integral of the first peak, for increasing (filled symbols) and decreasing (open symbols) pressures.

The hysteresis observed in the evolution of almost all XANES features, is also observed in the EXAFS features. Figure 2 shows the Fourier Transform (FT) of the experimental Mn K-edge EXAFS. The main peak contains information on the Mn coordination shell, its position corresponds to the average Mn-O bond length, not corrected for phase shifts. The amplitude of the first peak directly reflects the disorder within the Mn coordination shell. The restricted EXAFS k-range (8 Å^{-1}) characterizes a low-resolution study in R-space, where the Mn-O bond lengths are no longer distinguishable and the bond length distribution appears as a static contribution to the total disorder [10]. The increase in this peak integral (fig. 2, lower inset) corresponds to a decrease in the separation between long and short Mn-O bond lengths, *i.e.*, in the JT distortion. We identify three pressure ranges: a first one of slow increase ($P <$ 15 GPa), a second one of strong variation (15–25 GPa). Above 25 GPa the first peak in the Fourier transform are almost superimposed (FT at 26 GPa and 31 GPa on fig. 2), corresponding to a range of stabilization. The large double peak at 2–3 Å contains essentially the contributions of La single scattering and Mn-O-Mn multiple scattering. The relative intensities in this double peak vary notably in the first steps of the pressure increase ($P < 7$ GPa), then after only a global increase is observed. This indicates that the various mechanisms of inter-octahedra atomic accommodation (in particular octahedral tilts and La shifts) take place mainly in the low pressure regime. This is confirmed by the raise of the feature around 4.5 Å^{-1} in the EXAFS signal (fig. 2, upper inset) associated to octahedral tilt [11,17] and agrees with previous X-ray diffraction results [29]. We can deduce that, after an initial

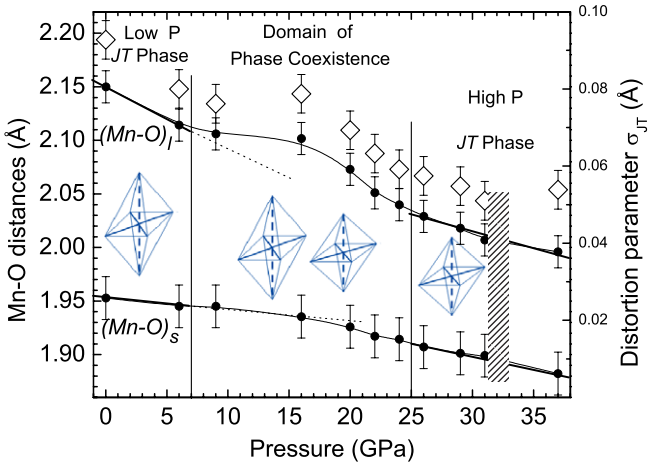

Fig. 3: (Colour on-line) Variation of the long $(\text{Mn-O})_l$ and short $(\text{Mn-O})_s$ bond lengths (plain circles) and distortion parameter (open diamonds) with increasing applied pressure. The onset of the metallic state is marked by an hatched zone.

octahedral rearrangement up to about 7 GPa, domains of a new phase with less distorted octahedra start to form and coexist with the initial phase up to 25 GPa, where only the second phase persists.

To assess the parameters of these less-distorted MnO_6 units, an overall quantitative analysis is done. For the EXAFS signal there is an enormous weight on the shortest interatomic distance occurring in the system, but no sensitivity to the long distance tail [36]. In a bimodal distribution with 4 short and 2 long distances, and given that the disorder associated to the long bond is larger than the disorder associated to the short bond [11], the two longer distances behave as a "tail" of the short bond signal. We checked the sensitivity of the EXAFS analysis to such "tail" by using the software Feff7 [37] to simulate the EXAFS signal given by Mn atoms in a distorted JT environment. Due to limited available k-range for the quantitative EXAFS analysis the standard gaussian EXAFS fitting procedure on the first peak of the Fourier transform gives a single distance at the value of the short one within an error of less than 0.02 Å, the longer distance contribution appearing as a slight increase in the disorder parameter. On the other hand, in the XANES range, the relationship between the reduction δR of the long bond length and the associated edge shift δE is rather linear [31] and allows a fair evaluation of the long-bond shortening with increasing pressure. From the edge shift (1.5 eV) a maximum of ≈ 0.15 Å is deduced. Figure 3 reports the evolution of the long and short bond lengths in the MnO_6 octahedra, obtained by this combined XANES and EXAFS analysis. In the low pressure regime ($P < 7$ GPa), the phase with highly JT distorted octahedra is present as a single phase. In this phase the reduction of the bond length with pressure is anisotropic and the JT distortion rapidly decreases. This reproduces essentially what has been reported by previous experiments [12,13,29] The evolution of the short distance in the range 0–6 GPa is in good agreement with the evolution of the average of the two shortest distance found by Loa and coworkers [12]. For the long distance, except the value at 0 GPa —found larger in diffraction meaurement— the agreement is also reasonable. The largest differences are found above 7 GPa. The long bond found in the diffraction analysis keeps dropping strongly, while in the XAS analysis, the decrease is retarded in the domain where the hysteresis loop denounces a phase coexistence. Taking as coherent distortion parameter σ_{JT}, defined as: $\sigma_{JT} = \sqrt{\frac{1}{6}\sum(Ri - R_0)^2}$, with R_i individual distances and R_0 average distance within the coordination shell, we found at ambient pressure $\sigma_{JT} \approx 0.1$ Å and for $P = 35$ GPa $\sigma_{JT} \approx 0.05$ Å. In between the evolution of the distortion parameter is given by the open diamond shaped symbols in fig. 3. In the precedent XAS study [13] the data were limited in pressure and quality. By extrapolating the evolution of the JT distortion up to 30 GPa we guessed that the distortion could disappear. This extrapolation was certainly spoiled by the presence of a phase mixing above 7 GPa. In the present work the JT distortion parameter, that is an average parameter over the phases presents in the compounds, is found to drop more slowly. In the single phase present above 25 GPa, long and short Mn-O bond lengths are still very different and their compression is nearly isotropic. The bond length separation is almost unchanged with pressure. The MnO_6 units present a lower JT distortion. Pressure is less effective in reducing the JT distortion above 25 GPa. In the range 0–5 GPa, associated to the distorted phase, σ_{JT} drops by about 15%, *i.e.*, a pressure dependence of $\delta\sigma_{JT}/\delta P \approx 0.03$. Over the range 26–35 GPa, associated to the second phase, it decreases only by 0.005, *i.e.*, $\delta\sigma_{\text{JT}}/\delta P \approx 0.001$. Especially, it keeps unchanged across the pressure range around 32 GPa, where the IM, transition is expected (fig. 3, hatched area).

We should mention that from EXAFS measurements we are not *a priori* able to differentiate the small distortions due to JT effect from site distortions intrinsic to a *Pbnm* space group. However, the split preedge structure, discussed here below, is related to the lift of degeneracy of the $3d\,e_g$ and t_{2g} level by JT effect, and the positions of the split components keep unchanged over the whole pressure range. We can then reasonably associate the small distortion at high pressure to a reduced JT effect.

The present scenario is compatible with the recent Raman data where the evidence of mixed phases comes from the emergence of a new phonon peak and a gradual transfer of spectral weight from the initial JT-peak to the new one. The strongest evolution in our XAS data occurs within the 15 to 25 GPa range, which correlates to the reversal of the spectral weight between Raman peaks [18]. Nevertheless, we identify the new phase not as an undistorted but, as a less-distorted JT one.

As far as theoretical approaches are concerned, *ab initio* calculations using soft pseudo-potentials support the conservation of a local distortion up to IM transition

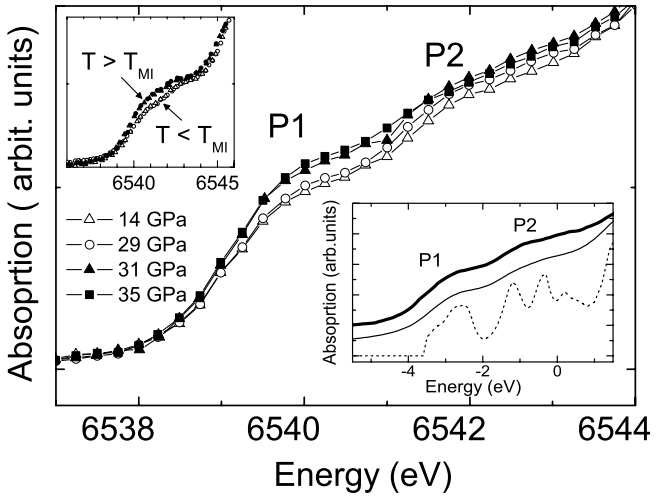

Fig. 4: Pre-edge features at increasing high pressures (open symbols $P < 30$ GPa, filled symbols $P > 30$ GPa). P1 and P2 peaks correspond, respectively, to transitions towards unoccupied e_g and t_{2g} states. Upper inset: pre-edge structure in $LaMnO_3$ around T_{IM} (open symbols: $T < T_{IM}$, filled symbols $T > T_{IM}$). Lower inset: comparison between experience (thick line) and *ab initio* calculations (thin line) of the pre-edge structures. The dotted line correspond to the calculation before convolution.

pressure [6,7,16,38]. Trimarchi and coworkers predicted the occurrence of a structural phase transition around 15 GPa leading to a situation with a mixture of poly-types of antiferromagnetic order [16]. Yamasaki and co-workers [6] claimed by combining local density approximations (LDA) and mean-field theories that both on-site repulsion (*d-d* correlation) and JT distortion are necessary for $LaMnO_3$ to be insulating below 32 GPa. More recently, Fuhr and coworkers [7] using LDA + U and a slave boson approach suggest close correlation between the IM transition and the JT local distortion; however, they do not completely exclude the possibility of a JT distorted metallic phase. These approaches have all been based on experimental structural data at limited pressures [12,13,29]. We give here a firm basis for further theoretical studies.

We turn now to the pre-edge structures. In $LaMnO_3$, it consists of two small peaks, assigned to dipole transition Mn 1*s* levels to 4*p* empty levels [39] (fig. 4). *Ab initio* simulations confirm that the quadrupole contribution is insignificant. 4*p*-3*d* hybridization for orbitals of the same Mn atom is forbidden due to the centrosymmetry of the Mn sites. However the 4*p* orbitals, having a large extension, hybridize with 3*d* orbitals of the Mn neighboring atoms. The structures at the pre-edge reflect then the 3*d* partial density of states. P_1 is associated to transitions to e_g majority states, and P_2 to transitions towards t_{2g} minority states. Actually the P_2 peak contains two main contributions, clearly evidenced in the derivative of the experimental spectrum (not shown) and well reproduced in the calculated spectra (fig. 4, lower inset). Experimentally, we do not observe any change in the pre-edge structure below 30 GPa. However, above 30 GPa, a small enhancement in the first peak intensity is detected. Such enhancement is also present across T_{IM} for temperature-induced metallization [11] (fig. 4, upper inset). Similar enhancements of the P_1 peak have also been reported in Ca-doped compounds [20,39,40]. It corresponds to an increase in the empty density of states associated to metallization. t_{2g} localized states being expected to participate much less to the charge transfer, no change is detected in P_2. One should also note that we do not observe any shift in the first peak position, in contrast with the observations of Chen and co-workers [41] in $TbMnO_3$. Such a shift, if it exists, should be lower than 0.1 eV. The enhancement of the P_1 structure provides an internal probe of the insulator-to-metal transition. Therefore, we can clearly confirm that the IM transition takes place, as expected, right above 30 GPa. It is then not directly associated to any structural change, specially it is unconnected with the symmetrization of the MnO_6 units.

In summary, we have investigated the local order in $LaMnO_3$ under applied pressure. The ambient phase with largely JT distorted MnO_6 units coexist over a large pressure range with a new phase with more regular but still JT distorted MnO_6 units. This latter phase is present alone above 25 GPa. No structural anomaly or singularity is observed in this pressure range. On the other hand, the IM transition around 32 GPa is fingerprinted from the XAS pre-edge structures. Our study provides evidences that the IM transition takes place in a distorted JT phase, without quenching of this distortion across the transition, which characterizes a unconventional Mott insulator. Insulator state and local distortion are not totally correlated and metallization should necessarily be driven by band overlap imposed by decreasing bond lengths under pressure.

* * *

We acknowledge financial support by the European Community for the experiments at SLS (Swiss Ligth Source).

REFERENCES

[1] Ahn C., Rabe K. and Triscone J., *Science*, **303** (2004) 488.
[2] Millis A. J., *Phys. Rev. B*, **53** (1996) 8434.
[3] Tyer R., Temmerman W. M., Szotek Z., Banach G., Svane A., Petit L. and Gehring G. A., *Europhys. Lett.*, **65** (2004) 519.
[4] Zenia H., Gehring G. A. and Temmerman W. M., *New J. Phys.*, **7** (2005) 257.
[5] Yin W.-G., Volja D. and Ku W., *Phys. Rev. Lett.*, **96** (2006) 116405.
[6] Yamasaki A., Feldbacher M., Yang Y.-F., Andersen O. K. and Held K., *Phys. Rev. Lett.*, **96** (2006) 166401.
[7] Fuhr J. D., Avignon M. and Alascio B., *Phys. Rev. Lett.*, **100** (2008) 216402.
[8] Pavarini E. and Koch E., *Phys. Rev. Lett.*, **104** (2010) 086402.

[9] Rodríguez-Carvajal J., Hennion M., Moussa F., Moudden A. H., Pinsard L. and Revcolevschi A., *Phys. Rev. B*, **57** (1998) R3189.

[10] Araya-Rodriguez E., Ramos A. Y., Tolentino H. C. N., Granado E. and Oseroff S., *J. Magn. & Magn. Mater.*, **233** (2001) 88.

[11] Souza R. A., Souza-Neto N. M., Ramos A. Y., Tolentino H. C. N. and Granado E., *Phys. Rev. B*, **70** (2004) 214426.

[12] Loa I., Adler P., Grzechnik A., Syassen K., Schwarz U., Hanfland M., Rozenberg G. K., Gorodetsky P. and Pasternak M. P., *Phys. Rev. Lett.*, **87** (2001) 125501.

[13] Ramos A. Y., Tolentino H. C. N., Souza-Neto N. M., Itié J.-P., Morales L. and Caneiro A., *Phys. Rev. B*, **75** (2007) 052103.

[14] Prado F., Zysler R., Morales L., Caneiro A., Tovar M. and Causa M. T., *J. Magn. & Magn. Mater.*, **196** (1999) 481.

[15] Qiu X., Proffen T., Mitchell J. F. and Billinge S. J. L., *Phys. Rev. Lett.*, **94** (2005) 177203.

[16] Trimarchi G. and Binggeli N., *Phys. Rev. B*, **71** (2005) 035101.

[17] Ramos A. Y., Tolentino H. C. N., Souza-Neto N. M., Caneiro A., Joly Y., Itie P., Flank A. M. and Lagarde P., *J. Phys.: Conf. Ser.*, **190** (2009) 012096.

[18] Baldini M., Struzhkin V. V., Goncharov A. F., Postorino P. and Mao W. L., *Phys. Rev. Lett.*, **106** (2011) 066402.

[19] Booth C. H., Bridges F., Kwei G. H., Lawrence J. M., Cornelius A. L. and Neumeier J. J., *Phys. Rev. B*, **57** (1998) 10440.

[20] Qian Q., Tyson T. A., Kao C.-C., Croft M., Cheong S.-W. and Greenblatt M., *Phys. Rev. B*, **62** (2000) 13472.

[21] Bridges F., Booth C. H., Anderson M., Kwei G. H., Neumeier J. J., Snyder J., Mitchell J., Garder J. S. and Brosha E., *Phys. Rev. B*, **63** (2001) 214405.

[22] Shibata T., Bunker B. A. and Mitchell J. F., *Phys. Rev. B*, **68** (2003) 024103.

[23] Sánchez M. C., García J., Subías G. and Blasco J., *Phys. Rev. B*, **73** (2006) 094416.

[24] Flank A., Cauchon G., Lagarde P., Bac S., Janousch M., Wetter R., Dubuisson J.-M., Idir M., Langlois F., Moreno T. and Vantelon D., *Nucl. Instrum. Methods B*, **246** (2006) 269.

[25] Morales L. and Caneiro A., *J. Solid State Chem.*, **170** (2003) 404.

[26] Shen Y., Kumar R. S., Pravica M. and Nicol M. F., *Rev. Sci. Instrum.*, **75** (2004) 4450.

[27] Klotz S., Chervin J.-C., Munsch P. and Le Marchand G., *J. Phys. D: Appl. Phys.*, **42** (2009) .

[28] Joly Y., *Phys. Rev. B*, **63** (2001) 125120.

[29] Pinsard-Gaudart L., Rodríguez-Carvajal J., Daoud-Aladine A., Goncharenko I., Medarde M., Smith R. I. and Revcolevschi A., *Phys. Rev. B*, **64** (2001) 064426.

[30] Natoli C., *Distance Dependence of Continuum and Bound State of Excitonic Resonance in X-Ray Absorption Near Edge Structure (XANES)* (Springer-Verlag) 1984, Chapt. 4, pp. 38–42.

[31] Souza-Neto N. M., Ramos A. Y., Tolentino H. C. N., Favre-Nicolin E. and Ranno L., *Phys. Rev. B*, **70** (2004) 174451.

[32] Zhao J., Angel R. J. and Ross N. L., *J. Appl. Crystallogr.*, **43** (2010) 743.

[33] Grunbaum N., Mogni L., Prado F. and Caneiro A., *J. Solid State Chem.*, **177** (2004) 2350.

[34] Souza J. A., Terashita H., Granado E., Jardim R. F., Oliveira N. F. and Muccillo R., *Phys. Rev. B*, **78** (2008) 054411.

[35] Cheng J.-G., Zhou J.-S., Goodenough J. B., Alonso J. A. and Martinez-Lope M. J., *Phys. Rev. B*, **82** (2010) 085107.

[36] Filipponi A., *J. Phys.: Condens. Matter*, **6** (1994) 8415.

[37] Rehr J. J., Mustre de Leon J., Zabinsky S. I. and Albers R. C., *J. Am. Chem. Soc.*, **113** (1991) 5135.

[38] Mizokawa T., Khomskii D. I. and Sawatzky G. A., *Phys. Rev. B*, **60** (1999) 7309.

[39] Bridges F., Booth C. H., Kwei G. H., Neumeier J. J. and Sawatzky G. A., *Phys. Rev. B*, **61** (2000) R9237.

[40] Ignatov A. Y., Ali N. and Khalid S., *Phys. Rev. B*, **64** (2001) 014413.

[41] Chen J. M., Chou T. L., Lee J. M., Chen S. A., Chan T. S., Chen T. H., Lu K. T., Chuang W. T., Sheu H.-S., Chen S. W., Lin C. M., Hiraoka N., Ishii H., Tsuei K. D. and Yang T. J., *Phys. Rev. B*, **79** (2009) 165110.